PHYSICAL REVIEW B **79**, 241304(R) (2009)

Distinct signatures for Coulomb blockade and Aharonov-Bohm interference in electronic Fabry-Perot interferometers

Yiming Zhang, D. T. McClure, E. M. Levenson-Falk, and C. M. Marcus
Department of Physics, Harvard University, Cambridge, Massachusetts 02138, USA

L. N. Pfeiffer and K. W. West
Bell Laboratories, Alcatel-Lucent Technologies, Murray Hill, New Jersey 07974, USA

(Received 31 December 2008; revised manuscript received 1 May 2009; published 3 June 2009)

Two distinct types of magnetoresistance oscillations are observed in two electronic Fabry-Perot interferometers of different sizes in the integer quantum Hall regime. Measuring these oscillations as a function of magnetic field and gate voltages, we describe three signatures that distinguish the two types. The oscillations observed in a 2.0 μm^2 device are understood to arise from a Coulomb blockade mechanism and those observed in an 18 μm^2 device from an Aharonov-Bohm mechanism. This work clarifies, provides ways to distinguish, and demonstrates control over these distinct mechanisms of oscillations seen in electronic Fabry-Perot interferometers.

DOI: 10.1103/PhysRevB.79.241304 PACS number(s): 73.43.Jn, 73.23.Hk

Mesoscopic electronics can exhibit wavelike interference effects,[1–4] particlelike charging effects,[5] or a complex mix of both.[6] Experiments over the past two decades have investigated the competition between wave and particle properties,[7] as well as regimes where they coexist.[6,8–10] The electronic Fabry-Perot interferometer (FPI)—a planar two-contact quantum dot operating in the quantum Hall regime—is a system where both interference and Coulomb interactions can play important roles. This device has attracted particular interest recently due to predicted signatures of fractional[11] and non-Abelian[12–14] statistics. The interpretation of experiments, however, is subtle, and must account for the interplay of charging and interference effects in these coherent confined structures.

The pioneering experimental investigation of resistance oscillations in an electronic FPI (Ref. 15) interpreted the oscillations in terms of an Aharonov-Bohm (AB) interference of edge states, attributing the magnetic field dependence of the field-oscillation period to a changing effective dot area. More recent experiments[16–19] have observed frequencies of integer multiples of the fundamental AB frequency; in particular, a proportionality of field frequency to the number of fully occupied Landau levels (LLs) has been well established[18–20] in devices up to a few μm^2 in size. Both experimental[17–19,21] and theoretical[20,22,23] investigations indicate that Coulomb interaction plays a critical role in these previously observed oscillations—as a function of both magnetic field and electrostatic gate voltage—suggesting an interpretation in terms of field- or gate-controlled Coulomb blockade (CB). The questions of whether it is even possible to observe resistance oscillations that arise from pure AB interference in FPIs, and if so, in what regime, and how to distinguish the two mechanisms, have yet to be answered to our knowledge.

In this Rapid Communication, we report two different types of resistance oscillations as a function of perpendicular magnetic field B and gate voltage in FPIs of two different sizes. The type observed in the smaller (2.0 μm^2) device, similar to previous results,[15–19,21] is consistent with the interacting CB interpretation, while that observed in the larger (18 μm^2) device is consistent with noninteracting AB interference. Specifically, three signatures that distinguish the two types of oscillations are presented. The magnetic field period is inversely proportional to the number of fully occupied LLs for CB, but field independent for AB; the gate-voltage period is field independent for CB, but inversely proportional to B for AB; resistance stripes in the two-dimensional plane of B and gate voltage have a positive (negative) slope in the CB (AB) regime.

The devices were fabricated on a high-mobility two-dimensional electron gas (2DEG) residing in a 30-nm-wide GaAs/AlGaAs quantum well 200 nm below the chip surface, with Si δ-doping layers 100 nm below and above the quantum well. The mobility is $\sim 2000\ m^2/Vs$ measured in the dark, and the density is $2.6\times 10^{15}\ m^{-2}$. Surface gates that define the FPIs are patterned using the electron-beam lithography on wet-etched Hall bars [see Fig. 1(a)]. These gates come in from top left and bottom right, converging near the middle of the Hall bar. Figures 1(b) and 1(c) show gate layouts for the 2.0 μm^2 and 18 μm^2 interferometers. All gate voltages except V_C are set ~ -3 V (depletion occurs at ~ -1.6 V). Voltages V_C on the center gates are set near 0 V to allow fine tuning of density and area.

Measurements are made using a current bias $I=400$ pA, with B oriented into the 2DEG plane as shown in Fig. 1(a). The diagonal resistance $R_D \equiv dV_D/dI$ is related to the dimensionless conductance of the device $g=(h/e^2)/R_D$.[24] Here, V_D is the voltage difference between edge states entering from the top right and bottom left of the device.

Figure 2(a) shows R_D as a function of B measured in the 2.0 μm^2 device, displaying several quantized integer plateaus. Figures 2(b) and 2(c) show the zoom ins below the $g=1$ and 2 plateaus, respectively, displaying oscillations in R_D as a function of B, with periods $\Delta B=2.1$ and 1.1 mT. This ΔB of 2.1 mT corresponds to one flux quantum $\phi_0 \equiv h/e$ through an area $A=2.0\ \mu m^2$, which matches the device design; hence 1.1 mT corresponds to $\phi_0/2$ through about the same area. This is indeed the field-period scaling observed previously,[15,18,19] where for f_0 number of fully occupied LLs in the constrictions, ΔB is expected to be given by $(\phi_0/A)/f_0$. Thus, in Fig. 3(a) we show ΔB at each $1/f_0$, and

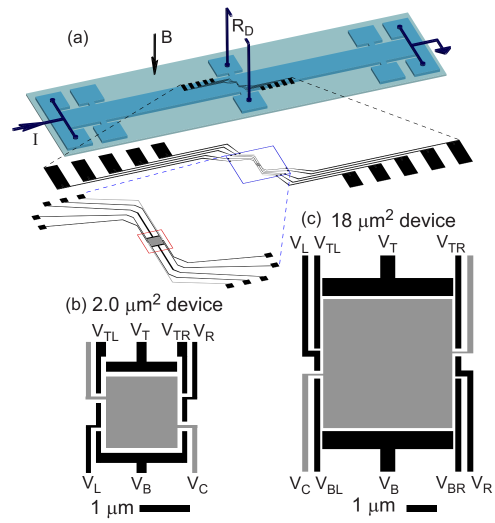

FIG. 1. (Color online) Measurement setup and devices. (a) Diagram of the wet-etched Hall bar, surface gates, and measurement configuration. Diagonal resistance R_D is measured directly across the Hall bar, with current bias I. Subsequent zoom ins of the surface gates are also shown; the red box encloses the detailed gate layouts for the device shown in (c). [(b) and (c)] Gate layouts for the 2.0 μm^2 and 18 μm^2 devices, respectively. The areas quoted refer to those under V_C.

a linear fit constrained through the origin, demonstrating the expected relationship.

We emphasize that this field-period scaling is inconsistent with simple AB oscillations, which would give a constant ΔB corresponding to one flux quantum through the area of the device. This can, however, be understood within an intuitive picture presented in a recent theoretical analysis[22] that considers a dominant Coulomb interaction within the device. In this picture, on the riser of R_D where $f_0 < g < f_0+1$, the

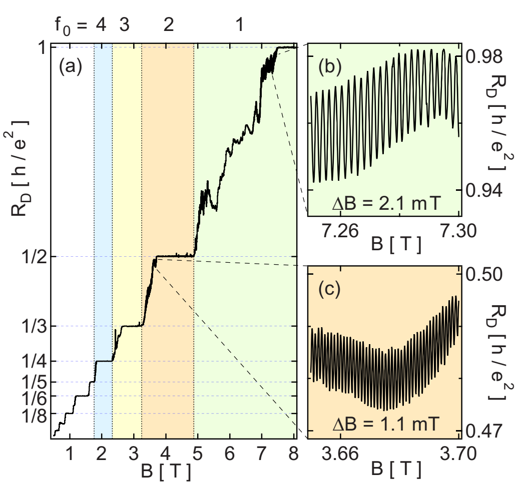

FIG. 2. (Color online) Oscillations in R_D as a function of magnetic field B for the 2.0 μm^2 device. (a) R_D as a function of B, showing well-quantized integer plateaus. Different colored backgrounds indicate different numbers of fully occupied LLs (f_0) through the device. [(b) and (c)] Zoom ins of the data in (a), at $f_0=1$ and 2, respectively, showing oscillations in R_D, and their B periods ΔB.

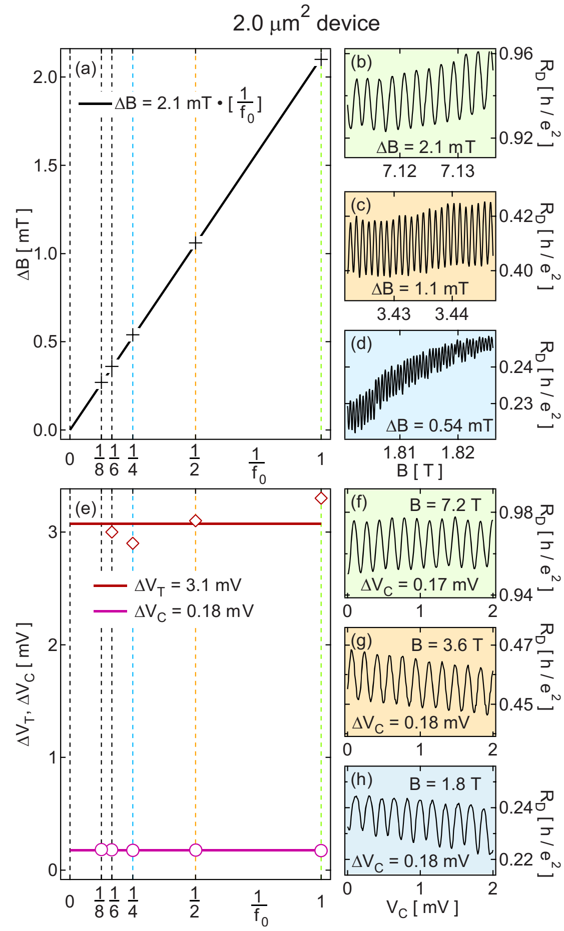

FIG. 3. (Color online) Magnetic field and gate-voltage periods at various f_0, for the 2.0 μm^2 device. (a) ΔB as a function of $1/f_0$ and a best-fit line constrained through the origin. [(b)–(d)] R_D oscillations as a function of B, at f_0=1, 2, and 4, respectively. (e) ΔV_T (diamonds) and ΔV_C (circles) as a function of $1/f_0$ and their averages indicated by horizontal lines. [(f)–(h)] R_D oscillations as a function of V_C, at f_0=1, 2, and 4, respectively.

(f_0+1)th and higher LLs will form a quasi-isolated island inside the device that will give rise to Coulomb blockade effects for sufficiently large charging energy,

$$E_C = \frac{1}{2C}(ef_0 \cdot BA/\phi_0 + eN - C_g V_{\mathrm{gate}})^2, \qquad (1)$$

where N is the number of electrons on the island, C is the total capacitance, and C_g is the capacitance between the gate and the dot. The magnetic field couples electrostatically to the island through the underlying LLs: when B increases by ϕ_0/A, the number of electrons in each of the f_0 underlying LLs will increase by one. These LLs will act as gates to the isolated island: Coulomb repulsion favors a constant total electron number inside the device, so N will decrease by f_0 for every ϕ_0/A change in B, giving rise to f_0 resistance oscillations.

Further evidence for the CB mechanism in the 2.0 μm^2 device is found in the resistance oscillations as a function of gate voltages. Figures 3(f)–3(h) show R_D as a function of

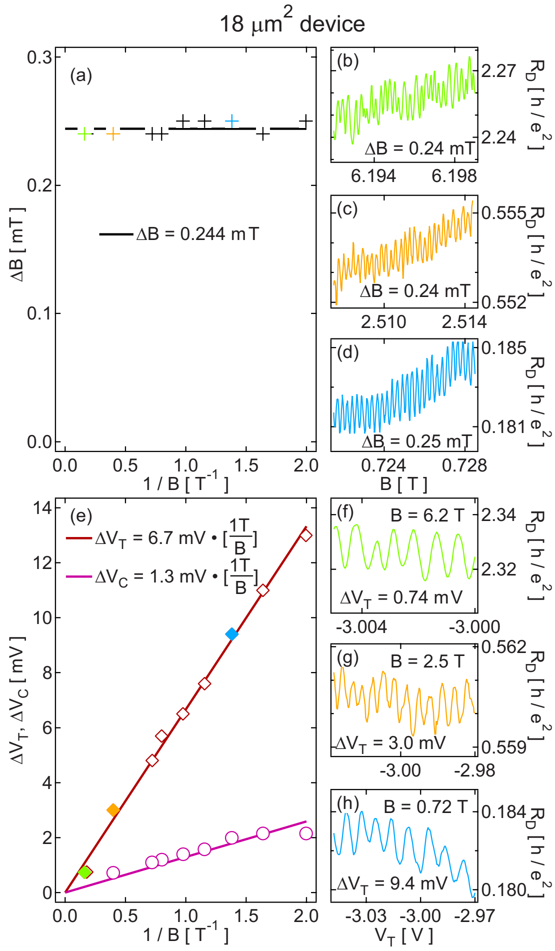

FIG. 4. (Color online) Magnetic field and gate-voltage periods at various B, for the 18 μm^2 device. (a) ΔB as a function of $1/B$ and their average indicated by a horizontal line. [(b)–(d)] R_D oscillations as a function of B over three magnetic field ranges. (e) ΔV_T (diamonds) and ΔV_C (circles) as a function of $1/B$ and best-fit lines constrained through the origin. [(f)–(h)] R_D oscillations as a function of V_T, at B=6.2 T, 2.5 T, and 0.72 T, respectively.

center gate voltage V_C, for f_0=1, 2 and 4, respectively. Figure 3(e) summarizes gate-voltage periods ΔV_T and ΔV_C at various f_0 and shows that they are independent of f_0. This behavior is consistent with the CB mechanism because, as can be inferred from Eq. (1), gate-voltage periods are determined by the capacitance C_g, which should be independent of f_0.

Having identified CB as the dominant mechanism[25] for resistance oscillations in the 2.0 μm^2 device, we fabricated and measured an 18 μm^2 device 1 order of magnitude larger in size, hence 1 order of magnitude smaller in charging energy. The center gate covering the whole device, not present in previous experiments,[15–19,21] also serves to reduce the charging energy. In this device, R_D as a function of B at three different fields is plotted in Figs. 4(b)–4(d), showing nearly constant ΔB. The summary of data in Fig. 4(a) shows that ΔB measured at ten different fields ranging from 0.5 to 6.2 T is indeed independent of B; its average value of 0.244 mT corresponds to one ϕ_0 through an area of 17 μm^2, close to the designed area. This is in contrast to the behavior observed in the 2.0 μm^2 device and is consistent with simple AB interference. Gate-voltage periods are also studied, as has been done in the 2.0 μm^2 device. Figures 4(f)–4(h) show R_D as a function of V_T at three different fields and Fig. 4(e) shows both ΔV_T and ΔV_C as a function of $1/B$. In contrast to the behavior observed in the 2.0 μm^2 device, ΔV_T and ΔV_C are no longer independent of B but proportional to $1/B$. This behavior is consistent with AB interference because the total flux is given by $\phi=B\cdot A$ and the flux period is always ϕ_0; assuming that the area changes linearly with gate voltage, gate-voltage periods would scale as $1/B$ for AB.

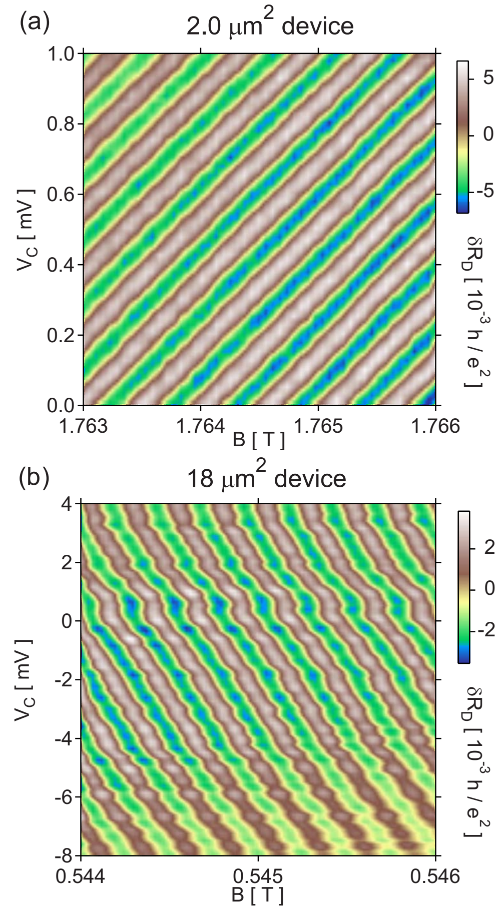

FIG. 5. (Color online) (a) δR_D, i.e., R_D with a smooth background subtracted, as a function of B and V_C, for the 2.0 μm^2 device. (b) Same as in (a), but for the 18 μm^2 device.

As shown above, the magnetic field and gate-voltage periods have qualitatively different B dependence in the 2.0 μm^2 and 18 μm^2 devices: the former consistent with CB, and the latter consistent with AB interference. Based on these physical pictures, one can make another prediction in which these two mechanisms will lead to opposite behaviors. In the CB case, increasing B increases the electron number in the underlying LLs, thus reducing the electron number in the isolated island via Coulomb repulsion. This is equivalent to applying more negative gate voltage to the device. On the other hand, for the AB case, increasing B increases the total flux through the interferometer and applying more positive gate voltage increases the area, thus also the total flux; therefore, higher B is equivalent to more positive gate voltage. As a result, if R_D is plotted in a plane of gate voltage and B, we expect stripes with a positive slope in the CB case and a negative slope in the AB case.

Figures 5(a) and 5(b) show R_D as a function of V_C and B for the 2.0 μm^2 and 18 μm^2 devices, respectively. As anticipated, the stripes from the 2.0 μm^2 device have a positive slope consistent with the CB mechanism, while stripes from the 18 μm^2 device have a negative slope consistent with AB interference. This difference can serve to determine the origin of resistance oscillations without the need to change the magnetic field significantly.

The three distinct signatures that we observe between AB interference and CB in this work can also shed light on some of the previous experiments and their interpretations. A few recent experiments studying fractional charge and statistics in FPIs (Refs. 26–28) interpret resistance oscillations as arising from AB interference while taking each gate-voltage period as indicating a change in a quantized charge. However, as shown in Fig. 4(e), the gate-voltage periods observed in the big device change by more than 1 order of magnitude over the field range that we study, and are inversely proportional to $1/B$, suggesting that charge is not quantized in the AB regime. Also in Ref. 27, the authors have observed that the magnetic field period stays constant between filling factor 1 and $\frac{1}{3}$, but the gate-voltage period at filling factor $\frac{1}{3}$ is only $\frac{1}{3}$ the size at filling factor 1. Although these observations can be interpreted as a result of fractional statistics, as the authors have done, there are at least two other possible interpretations: integer AB interference and CB with a charge of $e/3$. We consider clear identification of the mechanisms leading to oscillations—for instance, using the method of Fig. 5—to be crucial for interpreting future experiments, particularly, as the quantum states under investigation become more subtle.

We acknowledge J. B. Miller for device fabrication and discussion, R. Heeres for his work on the cryostat, and I. P. Radu, M. A. Kastner, B. Rosenow, N. Ofek, I. Neder, and B. I. Halperin for helpful discussions. This research is supported in part by Microsoft Corporation Project Q, IBM, NSF (Grant No. DMR-0501796), and the Center for Nanoscale Systems at Harvard University.

[1] *Mesoscopic Phenomena in Solids*, edited by B. L. Altshuler, P. A. Lee, and R. A. Webb (North-Holland, Amsterdam, 1991).

[2] W. Liang, M. Bockrath, D. Bozovic, J. H. Hafner, M. Tinkham, and H. Park, Nature (London) **411**, 665 (2001).

[3] Y. Ji, Y. Chung, D. Sprinzak, M. Heiblum, D. Mahalu, and H. Shtrikman, Nature (London) **422**, 415 (2003).

[4] P. Roulleau, F. Portier, D. C. Glattli, P. Roche, A. Cavanna, G. Faini, U. Gennser, and D. Mailly, Phys. Rev. B **76**, 161309(R) (2007).

[5] L. P. Kouwenhoven *et al.*, in *Mesoscopic Electron Transport*, edited by L. L. Sohn, L. P. Kouwenhoven, and G. Schon, NATO ASI Series E: Applied Science (Kluwer, Dordrecht, 1997), Vol. 345.

[6] I. L. Aleiner, P. W. Brouwer, and L. I. Glazman, Phys. Rep. **358**, 309 (2002).

[7] E. Buks, R. Schuster, M. Heiblum, D. Mahalu, and V. Umansky, Nature (London) **391**, 871 (1998).

[8] D. C. Glattli, C. Pasquier, U. Meirav, F. I. B. Williams, Y. Jin, and B. Etienne, Z. Phys. B **85**, 375 (1991).

[9] J. A. Folk, S. R. Patel, S. F. Godijn, A. G. Huibers, S. M. Cronenwett, C. M. Marcus, K. Campman, and A. C. Gossard, Phys. Rev. Lett. **76**, 1699 (1996).

[10] S. M. Cronenwett, S. R. Patel, C. M. Marcus, K. Campman, and A. C. Gossard, Phys. Rev. Lett. **79**, 2312 (1997).

[11] C. de C. Chamon, D. E. Freed, S. A. Kivelson, S. L. Sondhi, and X. G. Wen, Phys. Rev. B **55**, 2331 (1997).

[12] A. Stern and B. I. Halperin, Phys. Rev. Lett. **96**, 016802 (2006).

[13] P. Bonderson, A. Kitaev, and K. Shtengel, Phys. Rev. Lett. **96**, 016803 (2006).

[14] R. Ilan, E. Grosfeld, and A. Stern, Phys. Rev. Lett. **100**, 086803 (2008).

[15] B. J. van Wees, L. P. Kouwenhoven, C. J. P. M. Harmans, J. G. Williamson, C. E. Timmering, M. E. I. Broekaart, C. T. Foxon, and J. J. Harris, Phys. Rev. Lett. **62**, 2523 (1989).

[16] J. P. Bird, K. Ishibashi, Y. Aoyagi, and T. Sugano, Phys. Rev. B **53**, 3642 (1996).

[17] R. P. Taylor, A. S. Sachrajda, P. Zawadzki, P. T. Coleridge, and J. A. Adams, Phys. Rev. Lett. **69**, 1989 (1992).

[18] W. Zhou, F. E. Camino, and V. J. Goldman, AIP Conf. Proc. **850**, 1351 (2006); F. E. Camino, W. Zhou, and V. J. Goldman, Phys. Rev. B **76**, 155305 (2007).

[19] M. D. Godfrey, P. Jiang, W. Kang, S. H. Simon, K. W. Baldwin, L. N. Pfeiffer, and K. W. West, arXiv:0708.2448 (unpublished).

[20] M. W. C. Dharma-wardana, R. P. Taylor, and A. S. Sachrajda, Solid State Commun. **84**, 631 (1992).

[21] B. W. Alphenaar, A. A. M. Staring, H. van Houten, M. A. A. Mabesoone, O. J. A. Buyk, and C. T. Foxon, Phys. Rev. B **46**, 7236 (1992).

[22] B. Rosenow and B. I. Halperin, Phys. Rev. Lett. **98**, 106801 (2007).

[23] S. Ihnatsenka and I. V. Zozoulenko, Phys. Rev. B **77**, 235304 (2008).

[24] J. B. Miller, I. P. Radu, D. M. Zumbühl, E. M. Levenson-Falk, M. A. Kastner, C. M. Marcus, L. N. Pfeiffer, and K. W. West, Nat. Phys. **3**, 561 (2007).

[25] Although the existence of interference in small devices cannot be ruled out, we emphasize that Coulomb charging alone is sufficient to explain all data observed in small devices. A recent preprint [(P. V. Lin, F. E. Camino, and V. J. Goldman, arXiv:0902.0811 (unpublished)] interprets magneto-oscillations in a small dot in terms of an interfering AB path quantized to enclose an integer N. However, as will be seen in Fig. 4(e), gate-voltage periods can change continuously by 1 order of magnitude in the AB regime, suggesting that N is not quantized in the AB regime.

[26] F. E. Camino, W. Zhou, and V. J. Goldman, Phys. Rev. Lett. **95**, 246802 (2005); Phys. Rev. B **72**, 075342 (2005).

[27] F. E. Camino, W. Zhou, and V. J. Goldman, Phys. Rev. Lett. **98**, 076805 (2007).

[28] R. L. Willett, L. N. Pfeiffer, and K. W. West, arXiv:0807.0221 (unpublished).